Liquid crystal alignment in nanoporous anodic aluminum oxide layer for LCD panel applications

2010 Nanotechnology 21 285201

(http://iopscience.iop.org/0957-4484/21/28/285201)

Nanotechnology **21** (2010) 285201 (10pp) doi:10.1088/0957-4484/21/28/285201

Liquid crystal alignment in nanoporous anodic aluminum oxide layer for LCD panel applications

Chitsung Hong[1], Tsung-Ta Tang[2], Chi-Yu Hung[3], Ru-Pin Pan[3] and Weileun Fang[1,4]

[1] Institute of NanoEngineering and MicroSystems, National Tsing Hua University, Hsinchu, Taiwan
[2] Department of Physics, National Tsing Hua University, Hsinchu, Taiwan
[3] Department of Electrophysics, National Chiao Tung University, Hsinchu, Taiwan
[4] Department of Power Mechanical Engineering, National Tsing Hua University, Hsinchu, Taiwan

E-mail: fang@pme.nthu.edu.tw

Received 8 April 2010, in final form 18 May 2010
Published 18 June 2010
Online at stacks.iop.org/Nano/21/285201

Abstract

This paper reports the implementation and integration of a self-assembled nanoporous anodic aluminum oxide (np-AAO) film and liquid crystal (LC) on an ITO–glass substrate for liquid crystal display (LCD) panel applications. An np-AAO layer with a nanopore array acts as the vertical alignment layer to easily and uniformly align the LC molecules. Moreover, the np-AAO nanoalignment layer provides outstanding material properties, such as being inorganic with good transmittance, and colorless on ITO–glass substrates. In this application, an LCD panel, with the LC on the np-AAO nanoalignment layer, is successfully implemented on an ITO–glass substrate, and its performance is demonstrated. The measurements show that the LCD panel, consisting of an ITO–glass substrate and an np-AAO layer, has a transmittance of 60–80%. In addition, the LCD panel switches from a black state to a bright state at 3 V_{rms}, with a response time of 62.5 ms. In summary, this paper demonstrates the alignment of LC on an np-AAO layer for LCD applications.

(Some figures in this article are in colour only in the electronic version)

1. Introduction

The liquid crystal display (LCD) has found many applications in consumer electronics, such as projectors, mobile displays, notebooks, touch displays, PC monitors, TV, etc. The electro-optic effects of liquid crystal (LC) play an important role in LCD applications. However, the LC molecules cannot be aligned on a bare substrate surface. Thus, the LC alignment layer is employed to control the orientation of the LC molecules, and the electro-optic LC performance can be improved by the LC alignment layer. However, the traditional polyimide (PI) film rubbing method [1] for the LC alignment layer faces the challenges of photo-stability, uniformity, static electricity, dust contamination, etc for large advanced LCD panel applications. Various LC alignment techniques have been investigated as alternatives for the PI rubbing approach. Photo-alignment [2–4], ion beam bombardment [5, 6], and plasma beam alignment [7–9] are some of the potential approaches of LC alignment; however alignment instability, materials stability, image sticking, and low anchoring [10–12] issues require consideration. In addition, surface morphology alignment techniques, such as micro/nanorubbing [13–15], nano-imprinting [16, 17], oblique evaporation of silicon oxide (SiOx) film [18, 19], and electron beam writing [20] have also been reported; however, these approaches have the problems of poor optical properties and a non-smooth LC alignment layer [21].

Nanoporous anodic aluminum oxide (np-AAO) film, with uniformly distributed and high-density nanoscale pores, is a promising material for various applications. The np-AAO film is batch fabricated under electrochemical anodization processes, which can control the dimensions

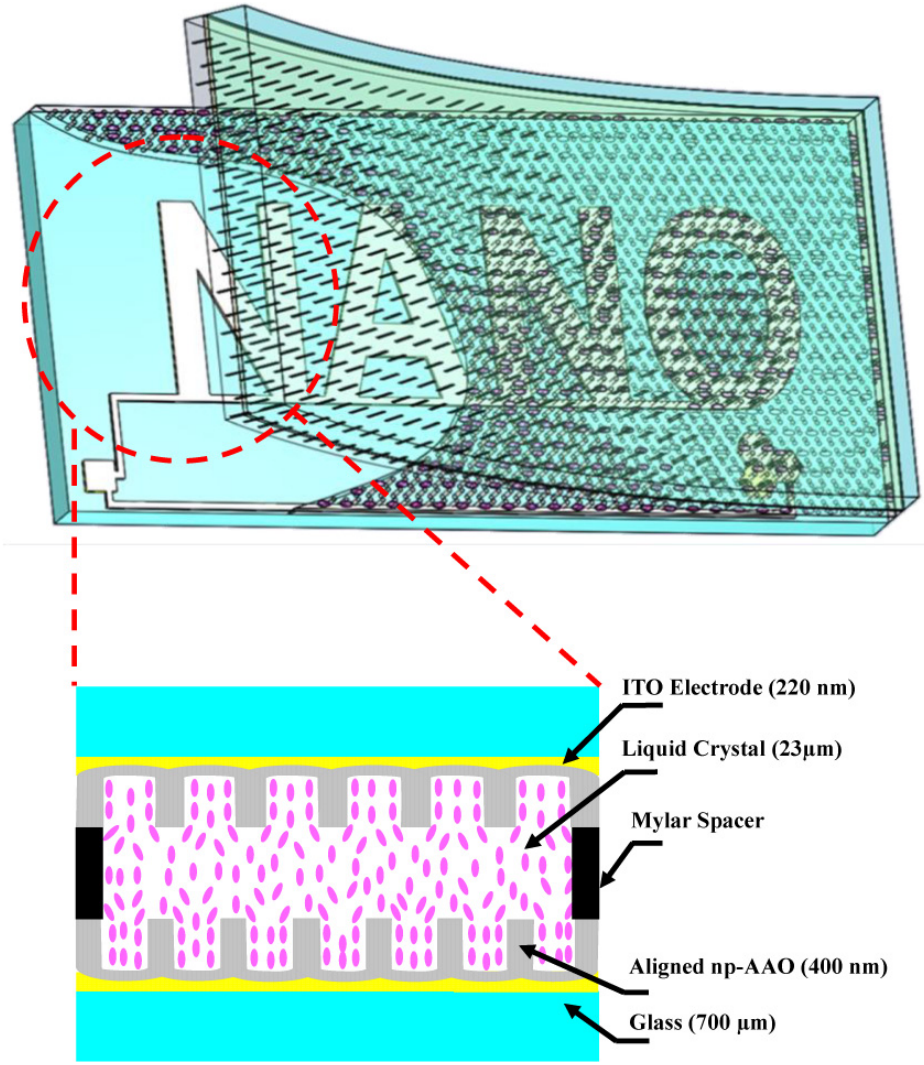

Figure 1. Schematic illustrations of the proposed np-AAO nanoalignment structure with LC for LCD panel application.

of the nanoscale pores [22–24]. The np-AAO consists of high-density and uniformly distributed nanopores, and is generally used as a template for the synthesis of various nanostructures [25, 26], nanomaterials [27, 28], and devices [29, 30], as the nanopores in ordinary np-AAO layer are parallel and isolated. Furthermore, the characteristics of transparency [31, 32], controllable optical properties [33–36], and photo- and mechanical-stabilities [37] provide an np-AAO film with additional advantages for optical applications. For instance, techniques that vertically align LC on np-AAO are reported [37, 38]. However, it remains a challenge to uniformly integrate a large area np-AAO nanoalignment layer with a conductive layer, such as a transparent ITO film, in order to form an LCD panel.

Processes that uniformly integrate a large area np-AAO on a conductive layer have been reported in [39, 40]. However, the issues of applications of large advanced LCD panels, namely, low transparency, optical loss, and materials compatibility cannot be ignored. Thus, this study presents a simple process to control and realize an inorganic np-AAO nanoalignment layer upon a transparent conductive layer for good LC alignment; in addition, it demonstrates the implementation of a self-assembled np-AAO film and LC on a ITO–glass substrate for LCD panel applications.

2. Design and fabrication

Figure 1 shows the architecture of the proposed LCD panel, which consists of two ITO coated glass substrates, with a self-assembled np-AAO layer, a Mylar spacer, and LC molecules. The LC between the ITO substrates is properly aligned by the np-AAO layer to realize the LCD panel application. The transmitting np-AAO film, with high-density and uniformly distributed nanoscale pores, can be directly fabricated by electrochemical processes on the top of the ITO–glass substrates. As the LC fills the space between the Mylar films and the np-AAO nanostructure, capillary force and gravity help to properly align the LC inside the nanopores [4, 41].

The fabrication processes, shown in figure 2, were established to implement the proposed device. First, two ITO–glass substrates were cleaned by ultrasonication in acetone, which were then treated by O_2-plasma (100 W at 26 °C for

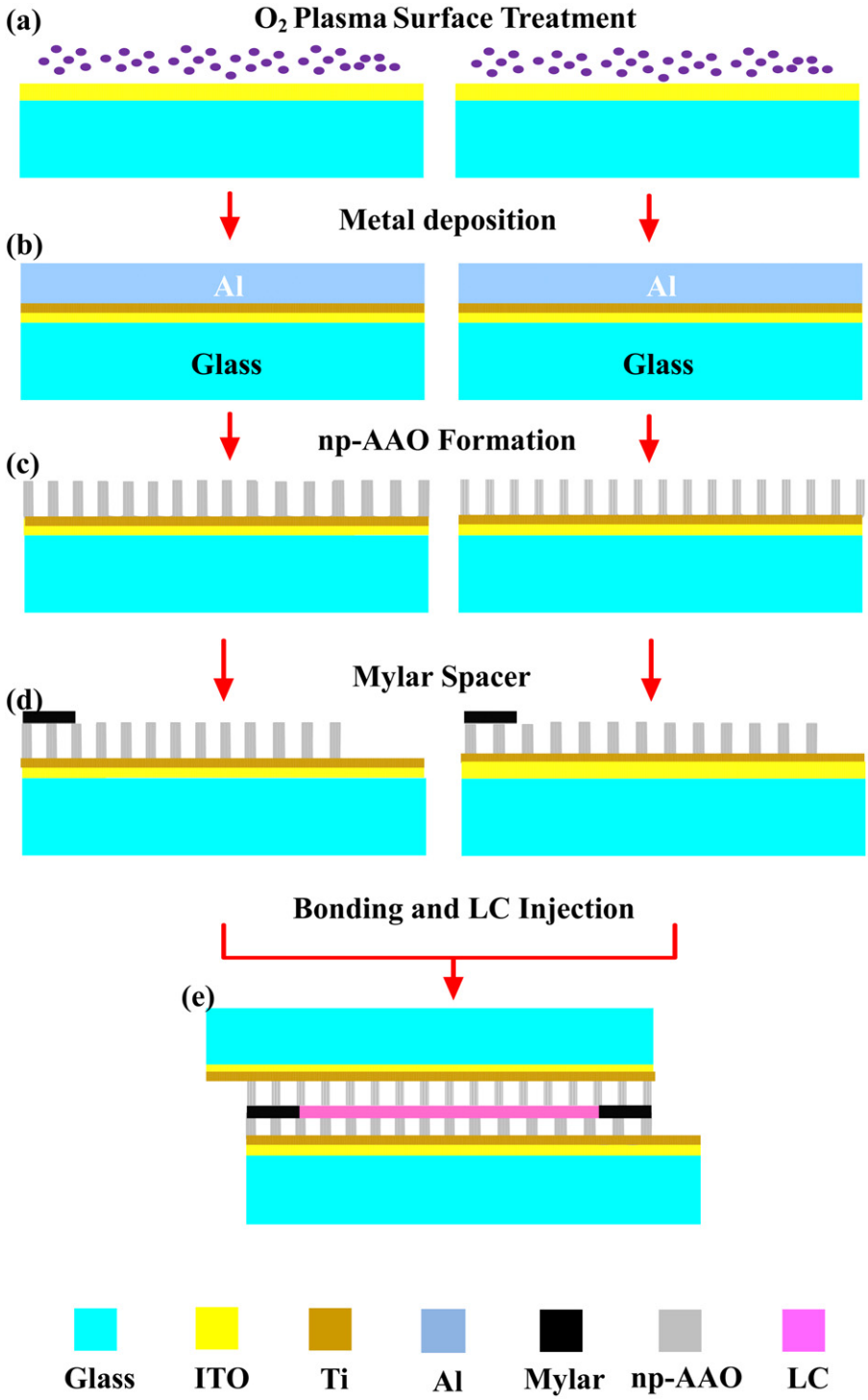

Figure 2. The fabrication process steps.

3 min), as shown in figure 2(a), thus, the adhesion between the ITO–glass substrate and the metal film deposited on its surface was improved. As illustrated in figure 2(b), a 500 nm thick Al and a 5 nm thick Ti layer, were respectively evaporated on the ITO–glass substrate. The Ti film was applied as adhesion for the Al film. Moreover, the Ti film acted as a passivation layer for the ITO layer during the following Al anodization process [39, 40]. As shown in figure 2(c), the np-AAO array was grown via the traditional two-step anodization of the Al film [22]. During the anodization process, the substrate was first immersed into a 12 °C aqueous solution with 0.3 M oxalic acid at 40 V DC voltage, and the np-AAO layer was formed on top of the Al/Ti film. The Al became 250 nm thick, and Ti remained 5 nm thick after the first anodization. Following this, the substrate was immersed in a mixture of chromic acid (1.8 wt%) and phosphoric acid (6 wt%) at 60 °C in order to remove the np-AAO formed on top of the Al/Ti film. Next, the substrate underwent a second anodization process, with

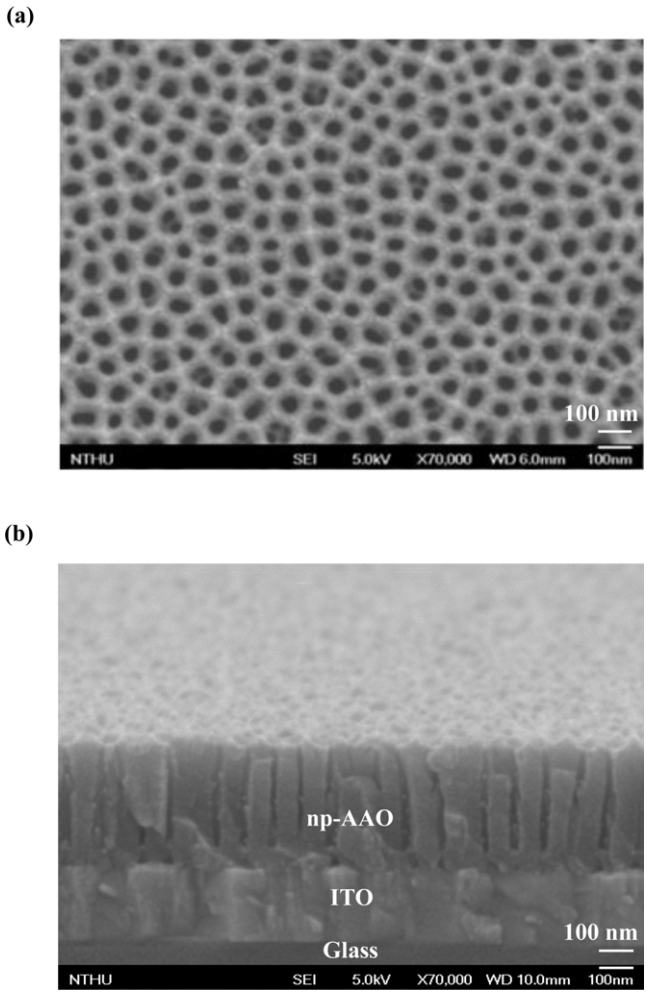

Figure 3. The FESEM micrographs of typical np-AAO layer fabrication results: (a) top view of the np-AAO array on ITO–glass, and (b) side view of the np-AAO array on ITO–glass.

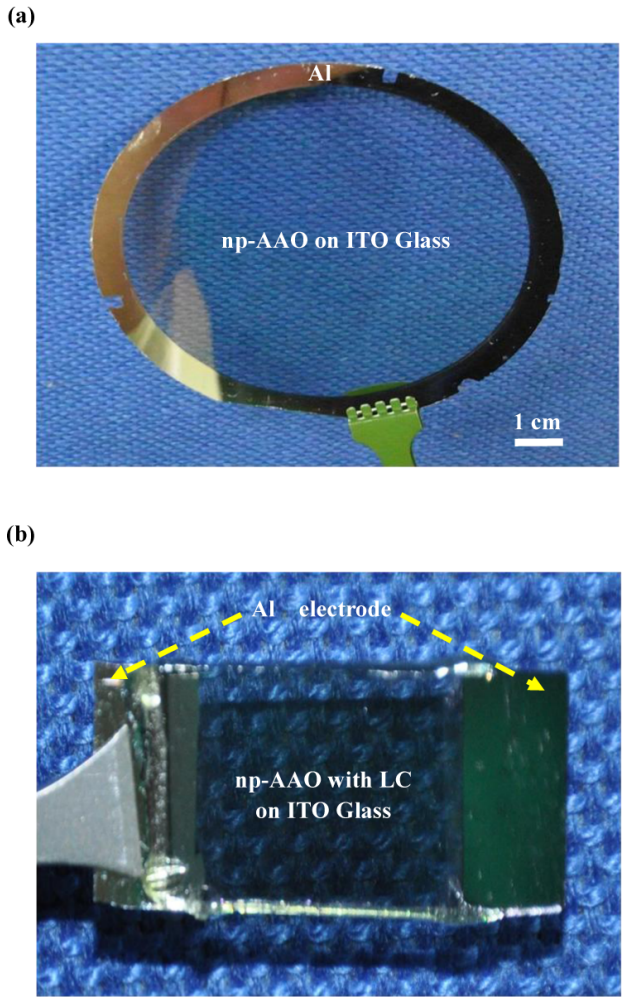

Figure 4. The photos of np-AAO on ITO–glass: (a) the np-AAO array on a 4-inch ITO–glass wafer, and (b) the LC filled into the ITO–glass substrate with the np-AAO nanoalignment layer to form the LCD panel.

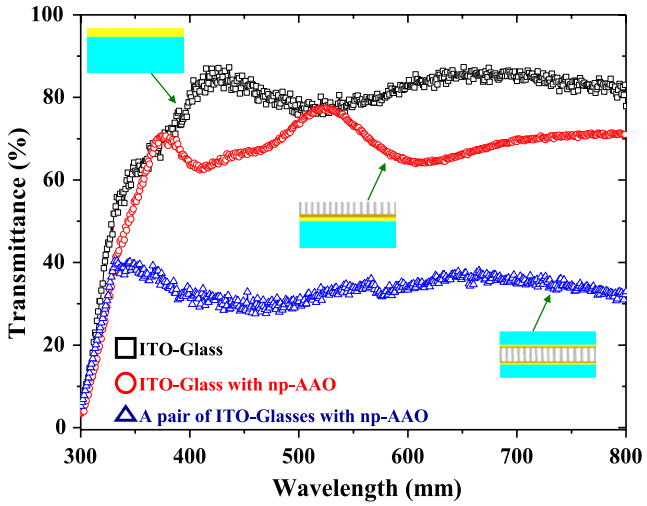

Figure 5. Characterization of the transmittance for ITO–glass with an np-AAO nanoalignment layer.

conditions the same as the first anodization step. The Al film remaining on the Ti/ITO–glass became transparent after being completely converted to the np-AAO, and the uniform distribution of the nanostructures were used for LC alignment. The Ti film became the passivation layer of the ITO, as the Al was completely converted to AAO. The Mylar film was patterned and placed on top of the np-AAO film, and after bonding of the two ITO–glass substrates acted as a spacer defining the filling-area of the LC, as shown in figure 2(d). Nematic LC, MLC-6608 (Merck Co.) was then injected into the area, where the np-AAO nanoalignment layer performed a uniform alignment of the LC. The LCD panel was achieved upon the injection-hole being sealed with glue, as shown in figure 2(e), and the ITO acted as the contact electrode.

A field emission scanning electron microscope (FESEM, JEOL 7000SF) was used to characterize the surface morphology of the np-AAO layer. The FESEM micrographs in figure 3(a) show the typical morphology of the np-AAO nanopore array. When the np-AAO layer is properly adhered to the ITO–glass, it is clearly observed from the side-view micrograph, as depicted in figure 3(b). Since the LC alignment is related to the surface morphology of the np-AAO layer, control of this process is critical in this study. Figure 4 demonstrates typical fabricated devices and their transparent characteristics. Figure 4(a) shows the transparent np-AAO

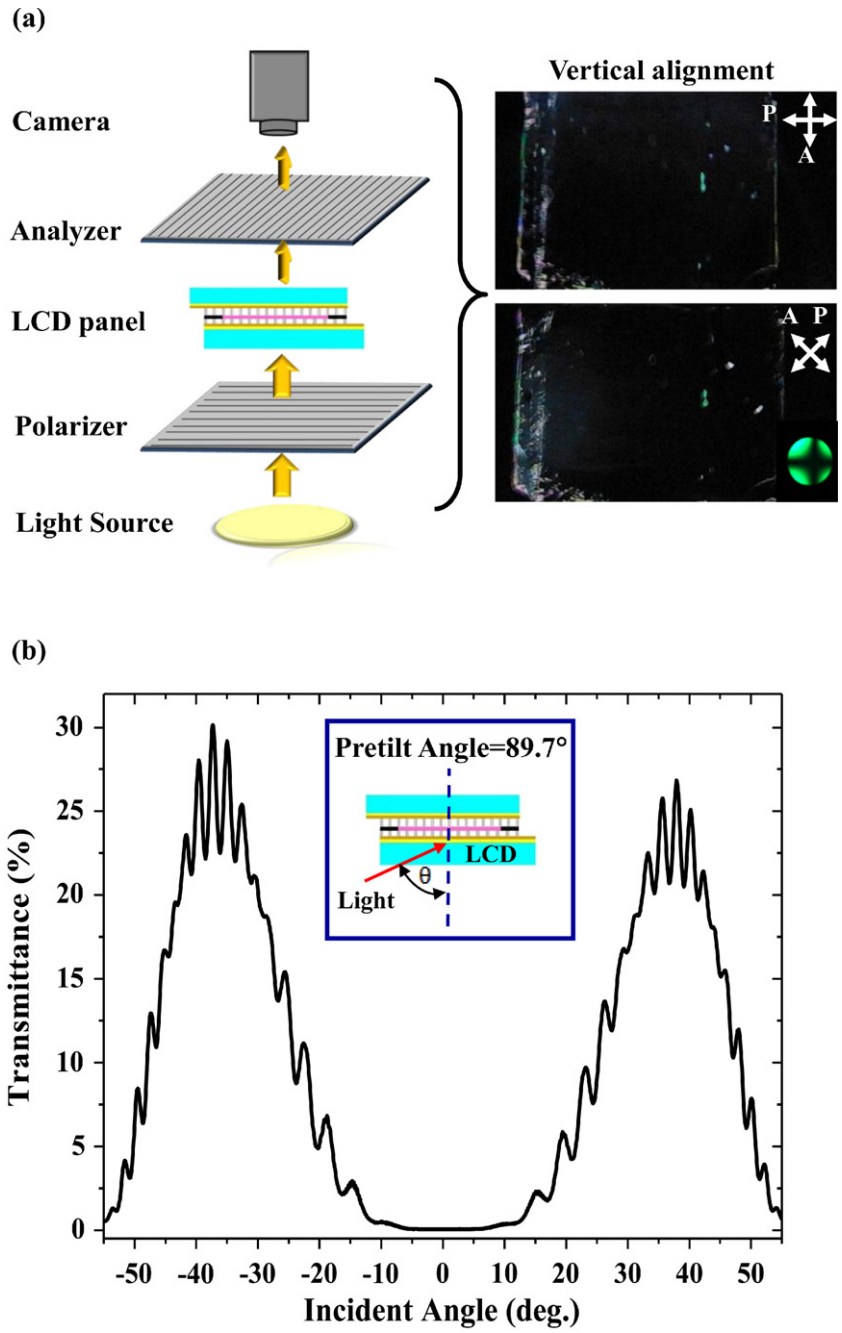

Figure 6. The LC alignment properties on np-AAO nanoalignment layer: (a) the scheme of the examination system and the transmitting images of the LC panel with an np-AAO nanoalignment layer, (b) the pre-tilted angle of LC alignment on an np-AAO nanoalignment layer.

layer on a 4-inch ITO–glass wafer. The Al layer pattern on the edge of the glass wafer is used as an electrode. np-AAO layers implemented on different size and shape transparent substrates are demonstrated. In addition, figure 4(b) shows a typical fabricated LCD panel after filling the LC into the ITO–glass with the np-AAO layer. The dimensions of the LCD panel are 3.9 cm × 1.2 cm × 0.14 cm.

3. Experimental results and discussion

To demonstrate the feasibility of the fabricated devices, the optical characteristics of the np-AAO alignment layer and the alignment of the LC on the np-AAO layer are characterized. An application of the np-AAO layer and LCD panel is demonstrated.

3.1. Optical characteristics of np-AAO nanoalignment layer

First, a UV–visible spectrometer (Ocean Optics, model ISS-UV-VIS and USB2000) was used to characterize the transmittance of np-AAO in order to show its performance in optical applications. Figure 5 shows the measured transmittance of ITO–glass with np-AAO for visible light (wavelength ranging from 300 to 800 nm). In these

measurements, the np-AAO layer with nanopores was recorded, and the bare ITO–glass was measured as a reference. Over a wavelength range of 300–800 mm, the transmittance of the ITO–glass with an np-AAO layer ranges between 60 and 80%. In comparison, the transmittance of ITO–glass substrates is around 80–90%. Moreover, the measurements in figure 5 also show the transmittance of a pair of stacked ITO glasses with an np-AAO layer is decreased to between 30 and 40%.

3.2. LC alignment

The alignment properties of the LC molecules on the np-AAO layers, without ITO conductive layers, have been demonstrated [38]. Since the LCs are filled into the uniform nanopore array of the np-AAO layer, which were parallel to the array walls, the LC molecules were vertically aligned. In this work, the LC alignment properties of np-AAO layers with ITO layers were examined using the figure 1 LCD panel, with crossed polarizers. Figure 6(a) shows the scheme of the examination system and the polarized images corresponding to the two orientations of the LCD panel, and at 45° to each other. For vertical LC alignment, the transmitting images in the crossed polarizers were always dark, regardless of the direction of the LCD panel. These dark states were observed in the LCD panel, with np-AAO nanoalignment layers, at both 0° and 45°, which indicates that excellent vertical alignment of the LC molecules is achieved. On the other hand, the conoscopic image of the LCD panel (the inserted image) shows a cross texture, and that the LC molecules are aligned vertically with the uniform np-AAO nanoalignment layer. To confirm the alignment properties of the LC molecules on the uniform np-AAO alignment layer, the pre-tilted angles of the LC molecules were measured using the crystal rotation method [42], as shown in figure 6(b). A pre-tilted angle of near 89.7° was obtained, indicating the vertical alignment of the LC molecules. The effect of multi-layer interference has been observed in small oscillations of transmittance by the LCD panel rotation. Moreover, this study also investigated the alignment of the LC molecules on np-AAO layers of different nanopore diameter. Three np-AAO layers with nanopore diameters of 35 ± 7 μm, 43 ± 5 μm, and 57 ± 9 μm were respectively fabricated and tested. The measurements in figure 7 show the pretilt angles of the LC molecules ranging from 87.7° to 89.5° for these three different nanopores sizes. Thus, the LC molecules are properly aligned by nanopores of 35–57 μm in diameter.

The conoscopic image in figure 8(a) shows a cross texture, which indicates a good vertical alignment of the LC at 0 V_{rms}; as the filled LC (MLC-6608, Merck Co.) was a negative LC, the LC molecules were aligned perpendicular to the external electric field. As shown in figure 8(a), the cross texture of the conoscopic images was shifted to the right by applying different voltages between 0 and 3 V_{rms} with a tungsten lamp with a green color filter, which demonstrates a good polarization modification of the LC molecules of an np-AAO nanoalignment layer by applying the voltage. Since the LC is uniformly aligned in the vertical direction, the LC molecules align in the same direction as the AC voltage

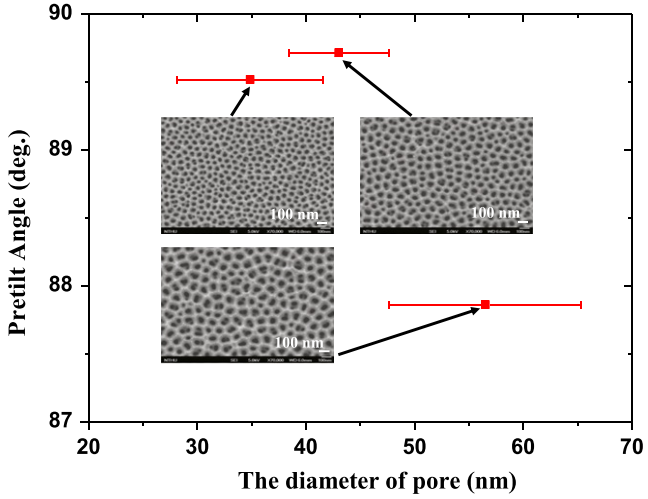

Figure 7. The pretilt angle of LC alignment on three np-AAO layers of different nanopore size.

applied to the device. Measurements show the LCD panel is changed from its dark to its bright state as the voltage increases from 0 to 2.6 V_{rms} (with a He–Ne laser as the light source), which indicates that the LC is properly aligned on the np-AAO layer. The estimated dependence of the transmittance of the LCD panel on applied voltage is shown in figure 8(b). The LC direction was controlled by the applied voltage, which estimates the phase retardation relationship between the transmittance T and phase retardation Γ is $T \propto \sin^2(\Gamma/2)$. By using this relationship, the phase retardation of the LC can be determined, as shown by the figure inserted in figure 8(b). According to the phase retardation, the Fréedericksz transition threshold voltage [43] was assessed as 2.19 V_{rms}; whereas, at 2.6 V_{rms}, the applied voltage was larger than the threshold voltage and the LC panel attains its bright state.

According to the polarized, conoscopic images and pre-tilted angle characteristics, uniform np-AAO layers with ITO conductive layers were also excellent candidates for the vertical alignment layers of the LCD application, and the vertical LC cells of these alignment layers were electrically controlled.

3.3. LCD application

The test setup in figure 9 was established for the functions of the fabricated LCD panel, with an np-AAO nanoalignment layer, as proposed by this study. The LCD test panel was placed between the polarizer and analyzer, with a white light lamp as a light source, and a camera to record the transmitted image of the LCD panel driven tests. Figure 10(a) shows the transmitted images under different driving voltages, which indicate that the LC molecule is uniformly aligned, according to the nanopores of the np-AAO layer, and thus, provides a bright state at 3 V_{rms} under a white light source. The results also indicate that the threshold voltage was around 2.2 V_{rms}, which agrees with the measurement in figure 8(b). The measurement in figure 10(b) shows that the typical response time of the LCD was 62.5 ms, as driven at a square waveform with an amplitude of 3 V_{rms} at

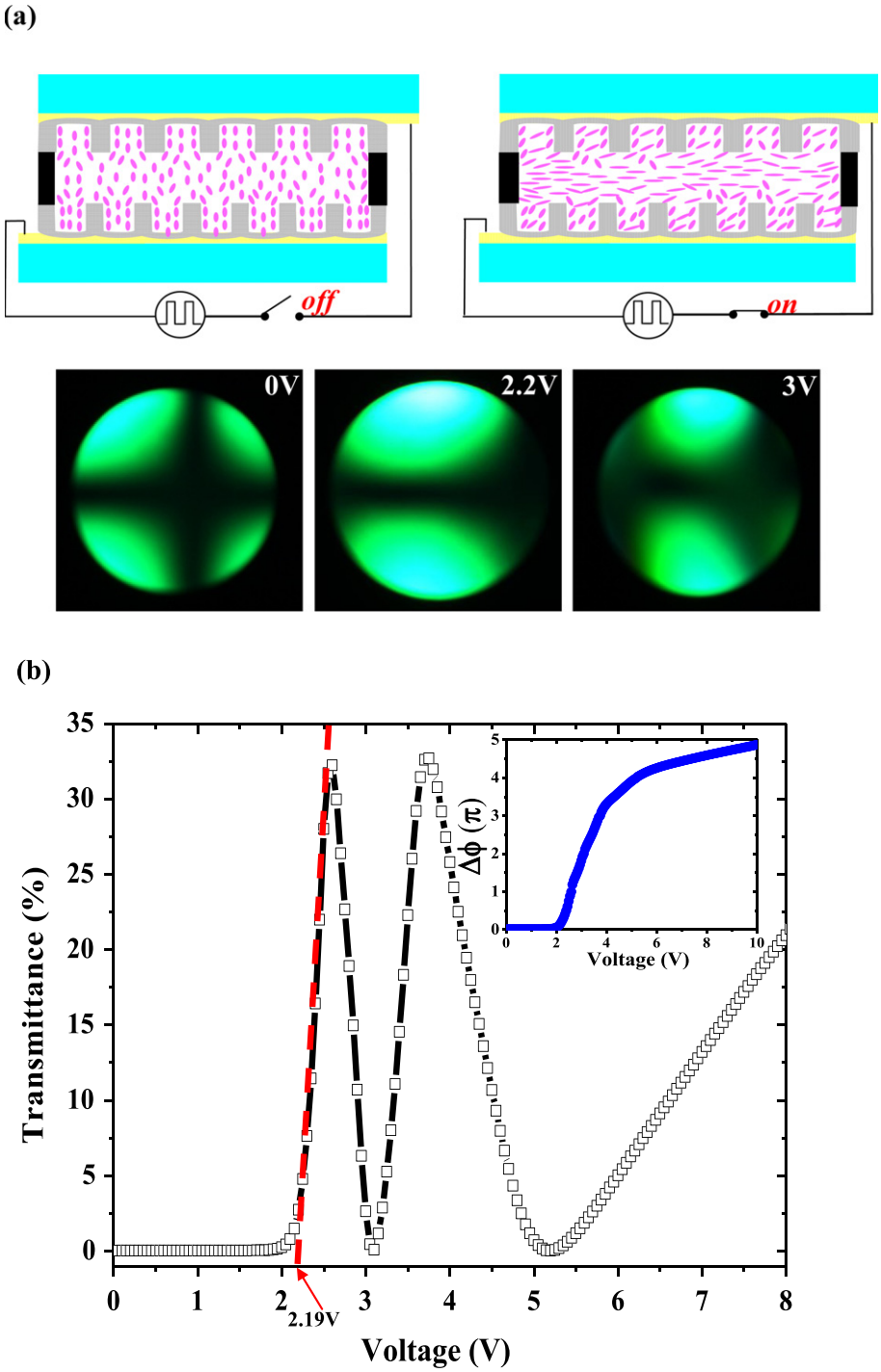

Figure 8. The scheme of LC alignment of the driving LC panel and its electro-optical properties: (a) the scheme of LC alignment and the conoscopic images with different applied voltage, (b) the transmittance and the phase retardation of the LC on the applied voltage.

a frequency of 1 kHz and period 1 s. The response time was further reduced with a reduced thickness of the LC (23 μm in this case), as defined by the Mylar spacer.

The test setup in figure 9 was employed to display the tests of the LCD panel. As indicated by the dashed lines in figure 9, a paper with colored letters was placed between the polarizer and the back light (with a white light as the light source) and the image on the LCD panel was recorded by the camera. The test was performed under an AC field with a square waveform at a frequency of 1 kHz, and voltage of 3 V_{rms}. The left photo in figure 11(a) shows the LCD panel as consisting of the ITO–glass and the np-AAO nanoalignment layer. As indicated in the photo, the dark region represents the np-AAO nanoalignment layer with the LC before applying the voltage. As the LC polarization was modulated by a 3 V_{rms} AC input voltage, the LCD panel changes to its bright state and the letters on paper were observed, as shown in the right photo of figure 11(a). This indicates that the LC

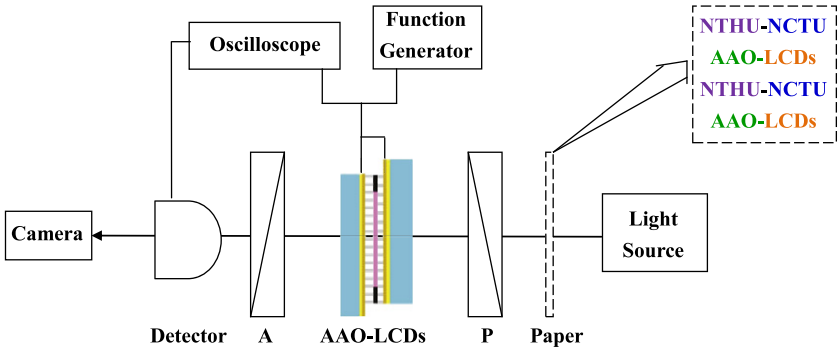

Figure 9. The measurement setup for the display testing of the LCD panel.

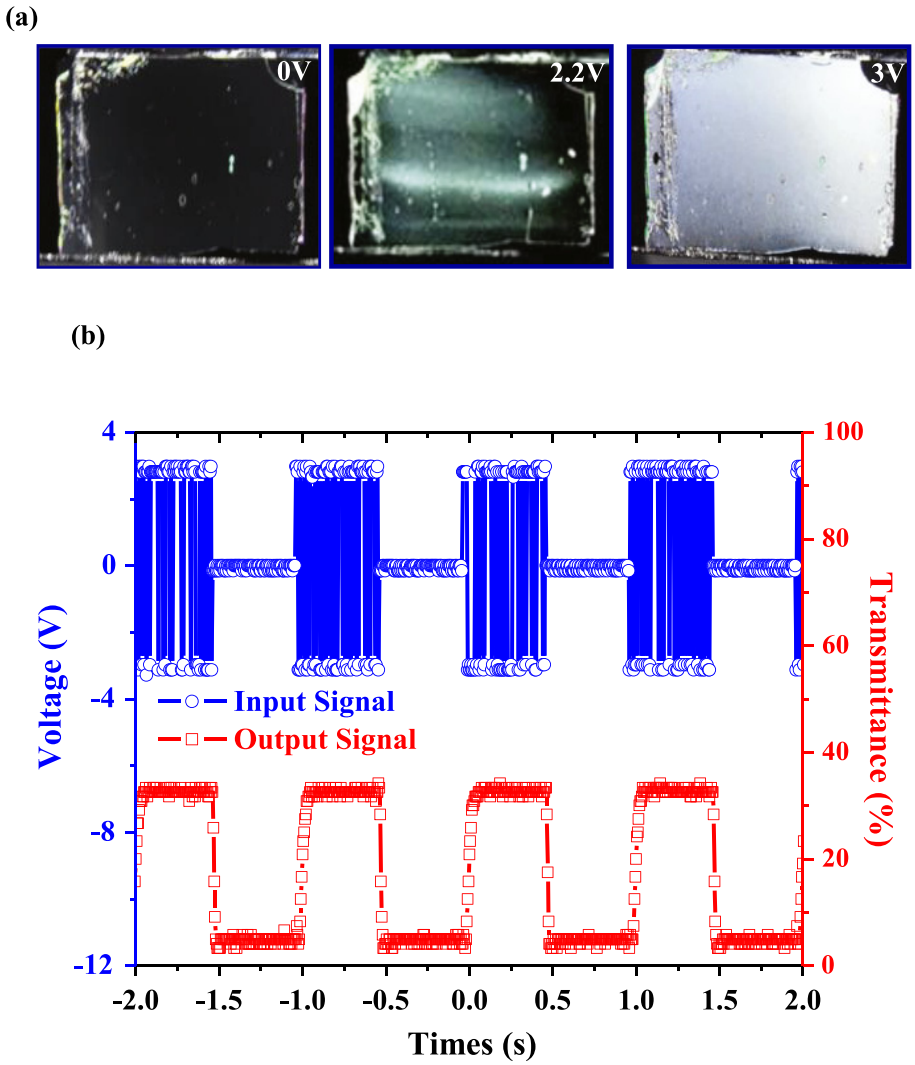

Figure 10. The typical measured electro-optical characteristics of the LCD panel with an np-AAO nanoalignment layer: (a) the voltage driving test showing 3 V_{rms} is required for the bright state, and (b) the response time is 62.5 ms.

molecules were uniformly aligned by the nanopores of the np-AAO nanoalignment layer, thus, these aligned LC molecules can move collectively in the same direction after applying a voltage that provides good transparency. This study also fabricated an LCD panel containing ITO-electrode patterns of 'NANO' characters and hexagon shapes, as illustrated in figure 1. Such an LCD panel is also in its black state prior to applying the voltage, as shown in the left photo of figure 11(b). As the driving voltage was applied to the ITO-electrode, only the LC above the ITO-electrode was switched from the black state to the bright state, and the characters and hexagon shapes were successfully displayed, as shown in the right photo of

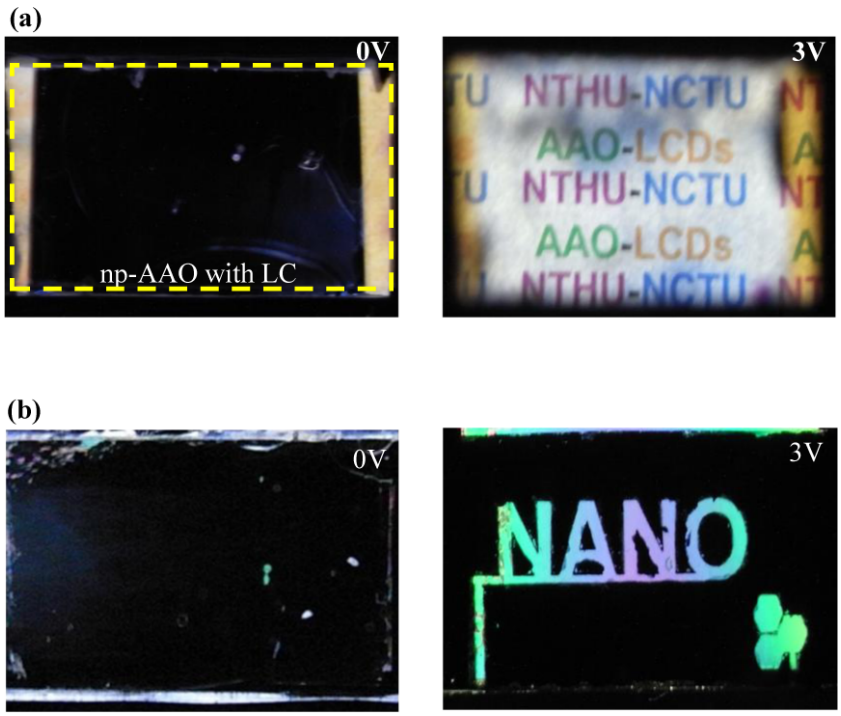

Figure 11. The display testing of the LCD panel using the test setup in figure 9: (a) the text on the paper in figure 9 appears after applying a 3 V_{rms} voltage to switch the LCD panel from the black state to the bright state, and (b) an LCD panel containing ITO-electrode patterns of 'NANO' characters (in figure 1) is used for test; the NANO characters appear as a 3 V_{rms} voltage is applied to the ITO-electrode.

figure 11(b). Thus, the feasibility of an np-AAO film as the alignment layer for an LCD application is demonstrated.

4. Conclusions

In summary, this paper successfully demonstrated the stacking of an np-AAO array with ITO conductive layers. The np-AAO was mainly prepared using O_2 plasma treated Ti/Al films, instead of a single Al layer, and by varying the process conditions, a high-density uniform np-AAO array can be grown on an ITO layer. The pre-tilted angle of the LC molecules is very close to 90° after using the np-AAO film as the alignment layer. Thus, the LC molecules can be vertically aligned on a uniform np-AAO layer with a conductive ITO film underneath. The measurements show that the LCs exhibit good electro-optical performance with the assistance of a uniform np-AAO nanoalignment layer. The threshold voltage of the LC is around 2.2 V_{rms}, and the typical response time of the LCD is 62.5 ms, as driven at a square waveform and an amplitude 3 V_{rms}. Because the anodizing process is a clean and controllable process, and the np-AAO layer is an inorganic, optically- and mechanically stable layer, the np-AAO nanostructure is a promising alignment layer for LCD panel applications.

Acknowledgments

This paper was partially supported by the National Science Council of Taiwan, under contract NSC 98-2221-E-007-003-MY3 and NSC 96-2221-E-009-131-MY3. The authors also appreciate Nanotechnology, Materials Science, and Microsystems, of the National Tsing Hua University (Taiwan), and the National Chiao Tung University (Taiwan) for providing fabrication facilities. The authors also greatly appreciate Professor K-C Hwang of the National Tsing Hua University (Taiwan) for preparing the FESEM micrographs.

References

[1] Nakamura N 1981 Surface topography and alignment of liquid crystal on rubbed oxide surface *J. Appl. Phys.* **52** 4561–7
[2] Gibbons W, Shannon P, Sun S T and Swetlin B 1991 Surface-mediated alignment of nematic liquid crystals with polarized laser light *Nature* **351** 49–50
[3] Andrienko D, Kurioz Y, Reznikov Y, Rosenblatt C, Petschek R, Lavrentovich O and Subacius D 1998 Tilted photo-alignment of a nematic liquid crystal induced by a magnetic field *J. Appl. Phys.* **83** 50–5
[4] Kim J K, Choi C J, Park J S, Jo S J, Hwang B H, Jo M K, Kang D, Lee S J, Kim Y S and Baik H K 2008 Orientational transition of liquid crystal molecules by a photoinduced transformation process into a recovery free silicon oxide layer *Adv. Mater.* **20** 3073–8
[5] Chaudhari P, Lacey J, Lien S A and Speidell J 1998 Atomic beam alignment of liquid crystal *Japan. J. Appl. Phys.* **37** L55–6
[6] Chaudhari P *et al* 2001 Atomic-beam alignment of inorganic materials for liquid crystal displays *Nature* **411** 56–9
[7] Sprokel G J and Gibson R M 1977 Liquid crystal alignment produced by RF plasma deposited films *J. Electrochem. Soc.* **124** 559–61
[8] Sun Z M, Engels J M, Dozov I and Durand G 1994 Ar+ beam sputtering on solid surfaces and nematic liquid crystal orientation *J. Physique* II **4** 59–73

[9] Watanabe R, Nakano T, Satoh T, Hatoh H and Ohki Y 1987 Plasma-polymerized films as orientating layers for liquid crystals *Japan. J. Appl. Phys.* **26** 373–6

[10] Chigrinov V, Muravski A, Kwok H S, Takada H, Akiyama H and Takatsu H 2003 Anchoring properties of photoaligned azo-dye materials *Phys. Rev.* E **68** 06172

[11] Yaroshchuk O, Kyrychenko V, Tao Du, Chigrinov V, Kwok H S, Hasebe H and Takatsu H 2009 Stabilization of liquid crystal photoaligning layers by reactive mesogens *Appl. Phys. Lett.* **95** 021902

[12] Kurihara R, Furue H, Takahashi T, Yamashita T, Xu J and Kobayashi S 2001 Fabrication of defect-free ferroelectric liquid crystal displays using photoalignment and their electrooptic performance *Japan. J. Appl. Phys.* **40** 4622–5

[13] Berreman D W 1972 Solid surface shape and the alignment of an adjacent nematic liquid crystal *Phys. Rev. Lett.* **28** 1683–6

[14] Kim J H, Yoneya M, Yamamoto J and Yokoyama H 2002 Nano-rubbing of a liquid crystal alignment layer by an atomic force microscope: a detailed characterization *Nanotechnology* **13** 133–7

[15] Varghese S, Crawford G P, Bastiaansen C W M, de Boer D K G and Broer D J 2004 Microrubbing technique to produce high pretilt multidomain liquid crystal alignment *Appl. Phys. Lett.* **85** 230–2

[16] Gwag J S, Oh-e M, Kim K R, Cho S H, Yoneya M, Yokoyama H, Satou H and Itami S 2008 A functionally separated nanoimprinting material tailored for homeotropic liquid crystal alignment *Nanotechnology* **19** 395301

[17] Park S, Padeste C, Schift H, Gobrecht J and Scharf T 2005 Chemical nanopatterns via nanoimprint lithography for simultaneous control over azimuthal and polar alignment of liquid crystals *Adv. Mater.* **17** 1398–401

[18] Janning L 1972 Thin film surface orientation for liquid crystal *Appl. Phys. Lett.* **21** 173–4

[19] Kim K C, Ahn H J, Kim J B, Hwang B H and Baik H K 2005 Novel alignment mechanism of liquid crystal on a hydrogenated amorphous silicon oxide *Langmuir* **21** 11079–84

[20] Kagajyo T, Fujibayashi K, Shimamura T, Okada H and Onnagawa H 2005 Alignment of nematic liquid crystal molecules using nanometer-sized ultrafine patterns by electron beam exposure method *Japan. J. Appl. Phys.* **44** 578–81

[21] Kim J B *et al* 2008 The directional peeling effect of nanostructured rigiflex molds on liquid-crystal devices: liquid-crystal alignment and optical properties *Adv. Funct. Mater.* **21** 1340–7

[22] Masuda H and Fukuda K 1995 Ordered metal nanohole arrays made by two-step replication of honeycomb structure of anodic alumina *Science* **268** 1466–8

[23] Lee W, Ji R, Gösele U and Nielsch K 2006 Fast fabrication of long-range ordered porous alumina membranes by hard anodization *Nature Mater.* **5** 741–7

[24] Nielsch K, Choi J, Schwirn K, Wehrspohn R B, Kim H and Gösele U 2002 Self-ordering regimes of porous alumina: the 10% porosity rule *Nano Lett.* **2** 677–80

[25] Lee W, Schwirn K, Steinhart M, Pippel E, Scholz R and Gösele U 2008 Structural engineering of nanoporous anodic aluminium oxide by pulse anodization of aluminium *Nature Nanotechnol.* **3** 234–9

[26] Kim W H, Park S J, Son J Y and Kim H 2008 Ru nanostructure fabrication using an anodic aluminum oxide nanotemplate and highly conformal Ru atomic layer deposition *Nanotechnology* **19** 045302

[27] Huang Z, Zhang X, Reiche M, Liu L, Lee W, Shimizu T, Senz S and Gösele U 2008 Extended arrays of vertically aligned sub-10 nm diameter [100] Si nanowires by metal-assisted chemical etching *Nano Lett.* **8** 3046–51

[28] Perez I, Robertson E, Banerjee P, Lecordier L H, Son S J, Lee S B and Rubloff G W 2008 TEM-based metrology for HfO2 layers and nanotubes formed in anodic aluminum oxide nanopore structures *Small* **4** 1223–32

[29] Langhammer C, Schwind M, Kasemo B and Zoric L 2008 Localized surface plasmon resonances in aluminum nanodisks *Nano Lett.* **8** 1461–71

[30] Ding D and Chen Z 2007 A pyrolytic carbon-stabilized, nanoporous Pd film for wide-range H_2 sensing *Adv. Mater.* **19** 1996–9

[31] Chu S Z, Wada K, Inoue S and Todoroki S 2002 Formation and microstructures of anodic alumina films from aluminum sputtered on glass substrate *J. Electrochem. Soc.* **321** B321–7

[32] Chu S Z, Wada K, Inoue S and Todoroki S 2003 Fabrication and characteristics of nanostructures on glass by Al anodization and electrodeposition *Electrochim. Acta* **48** 3147–53

[33] Yao J, Liu Z, Liu Y, Wang Y, Sun C, Bartal G, Stacy A M and Zhang X 2009 Optical negative refraction in bulk metamaterials of nanowire *Science* **321** 930

[34] Wang B, Fei G T, Wang M, Kong M G and Zhang L D 2007 Preparation of photonic crystals made of air pores in anodic alumina *Nanotechnology* **18** 365601

[35] Wang X H, Akahane T, Orikasa H and Kyotani T 2007 Brilliant and tunable color of carbon-coated thin anodic aluminum oxide films *Appl. Phys. Lett.* **91** 011908

[36] Lutich A A, Gaponenko S V, Gaponenko N V, Molchan L S, Sokol V A and Parkhutik V 2004 Anisotropic light scattering in nanoporous materials: a photon density of states effect *Nano Lett.* **4** 1755–8

[37] Maeda T and Hiroshima K 2005 Vertically aligned nematic liquid crystal on anodic porous alumina *Japan. J. Appl. Phys.* **43** L1004–6

[38] Tang T T, Kuo C Y, Pan R P, Shieh J M and Pan C L 2009 Strong vertical alignment of liquid crystal on porous anodic aluminum oxide film *J. Disp. Technol.* **5** 350–4

[39] Musselman K P, Mulholland G J, Robinson A P, Schmidt-Mende L and MacManus-Driscoll J L 2008 Low-temperature synthesis of large-area, free-standing nanorod arrays on ITO/glass and other conducting substrates *Adv. Mater.* **20** 4470–5

[40] Foong R P, Sellinger A and Hu X 2008 Origin of the bottlenecks in preparing anodized aluminum oxide (AAO) templates *ACS Nano.* **2** 2250–6

[41] Lee S H, Park S H, Lee M H and Oh S T 2005 Homeotropically aligned nematic liquid crystal device locked by a polymer wall with wide viewing angle *Appl. Phys. Lett.* **86** 031108

[42] Scheffer T J and Nehring J 1977 Accurate determination of liquid crystal tilt bias angles *J. Appl. Phys.* **48** 1783–92

[43] Zhang S, Wen B, Keast S S, Neubert M E, Taylor P L and Rosenblatt C 2000 Fréedericksz transition in an anticlinic liquid crystal *Phys. Rev. Lett.* **84** 4140–3